NeuroImage 62 (2012) 137–146

Contents lists available at SciVerse ScienceDirect

NeuroImage

journal homepage: www.elsevier.com/locate/ynimg

Mechanisms mediating parallel action monitoring in fronto-striatal circuits

Christian Beste [a,*], Vanessa Ness [a], Carsten Lukas [b], Rainer Hoffmann [c], Sven Stüwe [c], Michael Falkenstein [d], Carsten Saft [c]

[a] Institute for Cognitive Neuroscience, Biopsychology, Ruhr-University Bochum, Germany
[b] Department of Radiology, St. Josef Hospital, Ruhr-University Bochum, Germany
[c] Department of Neurology, Huntington Centre NRW, St. Josef Hospital, Ruhr-University Bochum, Germany
[d] Leibniz Research Centre Dortmund, Aging and CNS Diseases, Germany

ARTICLE INFO

Article history:
Accepted 8 May 2012
Available online 14 May 2012

Keywords:
Event-related potentials
Huntington's disease
Parallel processing
Source localisation
Wavelet analysis

ABSTRACT

Flexible response adaptation and the control of conflicting information play a pivotal role in daily life. Yet, little is known about the neuronal mechanisms mediating parallel control of these processes. We examined these mechanisms using a multi-methodological approach that integrated data from event-related potentials (ERPs) with structural MRI data and source localisation using sLORETA. Moreover, we calculated evoked wavelet oscillations. We applied this multi-methodological approach in healthy subjects and patients in a prodromal phase of a major basal ganglia disorder (i.e., Huntington's disease), to directly focus on fronto-striatal networks. Behavioural data indicated, especially the parallel execution of conflict monitoring and flexible response adaptation was modulated across the examined cohorts. When both processes do not co-incide a high integrity of fronto-striatal loops seems to be dispensable. The neurophysiological data suggests that conflict monitoring (reflected by the N2 ERP) and working memory processes (reflected by the P3 ERP) differentially contribute to this pattern of results. Flexible response adaptation under the constraint of high conflict processing affected the N2 and P3 ERP, as well as their delta frequency band oscillations. Yet, modulatory effects were strongest for the N2 ERP and evoked wavelet oscillations in this time range. The N2 ERPs were localized in the anterior cingulate cortex (BA32, BA24). Modulations of the P3 ERP were localized in parietal areas (BA7). In addition, MRI-determined caudate head volume predicted modulations in conflict monitoring, but not working memory processes.

The results show how parallel conflict monitoring and flexible adaptation of action is mediated via fronto-striatal networks. While both, response monitoring and working memory processes seem to play a role, especially response selection processes and ACC–basal ganglia networks seem to be the driving force in mediating parallel conflict monitoring and flexible adaptation of actions.

Introduction

Cognitive processes related to the flexible adaptation and control of actions play a pivotal role in everyday life (Redgrave et al., 2010). With respect to the control of actions, two sets of cognitive functions are distinguished (Eppinger et al., 2007): One process refers to the implementation of task-appropriate behaviour and includes the up-dating and switching between tasks (e.g. Ridderinkhof et al., 2004; Smith and Jonides, 1999). The other process refers to the monitoring of behaviour (e.g. Botvinick et al., 2004) and is important when a conflict between response alternatives exists (e.g. Folstein and van Petten, 2008). It is well-known that each of these processes is mediated via fronto-striatal loops (e.g. Aron et al., 2003; Kehagia et al., 2009; van Veen and Carter, 2002). However, in most daily situations monitoring and flexible adaptation of behaviour demand cognitive resources in parallel, rather than consecutively. Despite of this it is unclear what fronto-striatal mechanisms may mediate such parallel execution of the abovementioned processes. This question is interesting against the background of current theories of fronto-striatal network function: Many computational theories conceptualize fronto-striatal networks by some kind of a 'winner-take-all' (WTA) network (Bar-Gad et al., 2003; Humphries et al., 2006; Plenz, 2003). This dynamic is constituted by mutually coupled medium spiny neuron (MSN) ensembles. The ensembles that fire the strongest will inhibit other MSN ensembles representing other, competing actions (Bar-Gad et al., 2003; Jung and Shim, 2011; Redgrave et al., 1999). These conceptions imply that parallel processing is only possible to some extend (Redgrave et al., 1999), depending on the ability to represent different action representations at the same

* Corresponding author at: Institute for Cognitive Neuroscience, Department of Biopsychology, Ruhr-Universität Bochum, Universitätsstrasse 150, D-44780 Bochum, Germany. Fax: +49 234 321 4377.
E-mail address: christian.beste@rub.de (C. Beste).

1053-8119/$ – see front matter © 2012 Elsevier Inc. All rights reserved.
doi:10.1016/j.neuroimage.2012.05.019

time in fronto-striatal networks and especially MSN ensembles. MSNs are affected in many basal ganglia disorders. A possible way to infer the role of fronto-striatal and MSN mechanism in parallel monitoring and flexible adaptation of behaviour is hence to test these functions in a basal ganglia disorder characterised by changes in these circuits. Here, especially the examination of Huntington's disease (HD), an autosomal dominant neurological disorder, expressing neurodegenerative changes in basal ganglia, thalamic and cortical structures (e.g. Kassubek et al., 2005; Rosas et al., 2008; Tabrizi et al., 2009), may be of relevance, since changes in MSNs are a hallmark of this disease (e.g. Cepeda et al., 2007; Thomas et al., 2011). These changes are already evident in the pre-manifest stage of the disease (Tabrizi et al., 2009) (i.e., when clinical symptoms are not yet developed). Examining groups suffering from basal ganglia disorders using surface-based EEG data, it is possible to infer on fronto-striatal mechanisms and networks (e.g. Beste et al., 2007, 2010a,c; Verleger et al., 2010; Willemssen et al., 2009, 2011). According to this, we opted to examine the neurophysiological mechanisms underlying parallel monitoring and flexible adaptation. To infer the role of fronto-striatal loops, we compared results from healthy subjects with results from pre-manifest HD gene mutation carriers (pre-HDs). We integrated neurophysiological parameters derived from event-related potentials (ERPs) with structural MRI volumetric measurements and complement this approach with source localisation analyses on the ERPs using sLORETA (Pascual-Marqui, 2002). Moreover, evoked wavelet oscillations were analysed and integrated with structural MRI data.

To examine the parallel execution of response conflict monitoring and flexible adaptation of actions, we combined a Stroop with a task-switching paradigm. Due to MSN neuron dysfunction in pre-HDs situations that primarily involve parallel conflict processing and task-switching may overstrain fronto-striatal circuits and should lead to declines in performance.

On a neurophysiological level, increasing degrees of response conflict have been shown to increase the N2 event-related potential (ERP), which has been shown to be modulated in its amplitude by the anterior cingulate cortex (ACC) (e.g. Folstein and van Petten, 2008; van Veen and Carter, 2002). Variations in the N2 also occur in task switching. Here, a reconfiguration process occurs that may involve attentional shifts, the retrieval of goals and rules from working memory, the activation of the relevant task set/inhibition of the irrelevant task set (e.g. Kiesel et al., 2010; Monsell, 2003) or resolving of interference from the previous trial (task-set inertia) (Allport et al., 1994; Wylie and Allport, 2000). These processes lead to longer response times (RTs), known as 'switch costs' (Rogers and Monsell, 1995). Switch costs affect the P3 ERP, which supposedly reflects increased demands on working memory during the implementation of a switch (Barcelo et al., 2006; Gehring et al., 2003; Karayanidis et al., 2003). It has been shown that efficient task-switching is related to an increased N2 and an attenuated P3 (Gajewski et al., 2010).

In particular, the N2 should be smaller and the P3 may be larger in pre-HDs than in healthy controls. At the level of neural oscillations, it has been shown that oscillations in the delta or theta frequency band are amplified in conditions, where demands on cognitive control and behavioural monitoring are high (Beste et al., 2007, 2010a; Ocklenburg et al., 2011; Yordanova et al., 2004). Oscillations in the delta and theta frequency band have been shown to be important for inhibitory processes (Ocklenburg et al., 2011) and are also supposed to play an important role in task switching (e.g. Monsell, 2003). Especially, oscillations in the theta frequency band are closely related to central executive and working memory processes (e.g. Hanslmayr et al., 2008; Sammer et al., 2007; Sauseng et al., 2010), as well as by the application of a Stroop paradigm (Hanslmayr et al., 2008). It is therefore possible that besides the delta frequency band, the theta frequency band reveals effects between groups. Pre-HDs are expected to be less able to increase delta or theta frequency band power during task switching, under high Stroop conflict. Group differences, observed for the N2 ERP and data, are expected to be localised in the ACC using sLORETA (review: Folstein and van Petten, 2008) and structural MRI-volumetric measures of the caudate head may correlate with electrophysiological and behavioural parameters. For the P3 ERP, parietal sources may underlie group differences as revealed by sLORETA analyses. The individual modulation of behavioural performance and neurophysiological processes in pre-HDs may further depend on their individual genetic disease load and proximity to the onset of disease manifestation (e.g. Tabrizi et al., 2009).

Materials and methods

Participants

A group of thirty (N = 30) right-handed, pre-manifest HD gene mutation carriers (pre-HDs), defined by a positive gene test, underwent neurological investigation. The pre-HDs were scored according to the Unified Huntington's disease Rating Scale (UHDRS) (Siesling et al., 1998) "motor score" (MS), "total functional capacity scale" (TFC) and "independence scale" (IS). They completed the verbal fluency test, symbol digit test, Stroop colour naming, Stroop word reading and Stroop interference test, which were summarised as "cognitive score" (CS) (Huntington Study Group, 1996). The "absence of clinical motor symptoms" was based on expert raters' assessments of motor signs, which were not sufficient for the diagnosis of HD (Diagnostic Confidence Level [DCL], item 17 of the UHDRS Motor Assessment) (Huntington Study Group, 1996). For each pre-HD participant the probability of estimated disease onset (eAO) within five years was calculated according to Langbehn's parametric model (Langbehn et al., 2004). Moreover, the expected age of onset (eAO) was estimated using Langbehn's and Ranen's formula (Ranen et al., 1995). For pre-HD subjects the years to disease onset (YTO) were calculated by subtracting the subject's age at the time of investigation from his or her eAO. Additionally, we calculated the "Disease burden score" (DBS = [CAG repeat − 35.5] age) for each subject (e.g. Tabrizi et al., 2009).

As controls, 30 right-handed, healthy subjects matched to the pre-HD group in age, sex, educational status and socio-economic background were enrolled in the study. All participants gave written informed consent, before the study protocols were commenced. The Ethics Committee of the Ruhr-University Bochum (Germany) approved the present study. Demographical information is given in Table 1.

Task

The task combines a Stroop paradigm with a switching paradigm (see also: Eppinger et al., 2007). The stimuli were four colour words

Table 1
Demographical data of the pre-manifest HD gene mutation carriers group and the healthy control group. The mean and standard deviation (SD) are given.

Parameter	Pre-HD	Control
N	30	30
Age	38.66 (10.54)	39.55 (8.9)
Sex	16 female/14 male	16 female/14 male
CAG	42.08 (1.78)	NA
Disease burden score (DBS)	253.5 (75.25)	NA
Years to onset (YTO) Ranen et al. (1995)	6.78 (7.74)	
Years to onset (YTO) Langbehn et al. (2004)	16.28 (8.1)	NA
5-year probability	16.18 (16.77)	NA
UHDRS motor score (MS)	2.76 (2.56)	NA
UHDRS total functional capacity scale (TFC)	12.9 (0.3)	NA
UHDRS independent scale (IS)	99.3 (1.7)	NA
UHDRS cognitive score (CS)	331 (39.45)	NA

(i.e., RED, BLUE, YELLOW and GREEN) (3×2 cm, or 3×2° visual angle at a viewing distance of 57 cm) presented at the centre of the screen for 300 ms. These colour words are presented either in a rhomb or in a square. These shapes serve as cue stimuli denoting the task rule. Cue and target stimulus are separated by a short delay of 150 ms. When a rhomb is presented, subjects are instructed to respond according to the 'colour rule'; when a square is presented the subjects respond according to the 'word rule'. The subjects respond using their index fingers to BLUE (left key press) and YELLOW (right key press). The middle fingers are used to respond to the RED (left middle finger) and GREEN colour (right middle finger). The stimuli are presented on the screen until the response is executed. For the 'colour rule' the subjects respond according to the print-colour of the word and ignore the meaning of the word (e.g. BLUE printed in green, subjects respond with the left index finger). For the 'word rule' subjects respond according to the meaning of the word and ignore the print-colour of the word. In the following sections, colour rule trials and word rule trials are referred to as 'incompatible' and 'compatible' trials respectively. The paradigm contains four different trial types, shown in Fig. 1: (i) non-switch, compatible [i.e., on two consecutive trials the font colour of the word corresponds to its meaning]; (ii) switch, compatible [i.e., on two consecutive trials the rule changes, with the font colour of the word corresponding to its meaning]; (iii) non-switch, incompatible trials [i.e., on two consecutive the font colour of the word does not correspond to its meaning]; and (iv) switch, incompatible trials [i.e., on two consecutive trials the rule changes and the font colour of the word does not correspond to its meaning].

The latter condition is the most difficult condition, since conflict monitoring and switching processes are required in parallel. The trial order is pseudo-randomized with each condition occurring equally frequent. After familiarising the patients and controls with the colour and the word task, the experiment was conducted. The experiment consists of 480 trials, with each of the four different trial types being presented in 120 trials. Participants were seated at a distance of 57 cm from the screen and had to fixate a black fixation cross that was presented in the middle of the screen throughout the experiment. After a response was executed the next trial was presented 1250 ms thereafter (jittered between 1000 and 1500 ms). During this period, only the central fixation cross was presented.

EEG recording and analysis

EEG was recorded from 65 Ag–AgCl electrodes at standard scalp positions against a reference electrode located at Cz. The sampling rate was 500 Hz. All electrode impedances were kept below 5 kΩ. Data processing involved a manual inspection of the data to remove technical artefacts. After manual inspection, a band-pass filter ranging from 0.5 to 20 Hz (48 dB/oct) was applied. After filtering, the raw data were inspected a second time. To correct for periodically recurring artefacts (pulse artefacts, horizontal and vertical eye movements) an independent component analysis (ICA; Infomax algorithm) was applied to the un-epoched data set. Afterwards, the EEG data was segmented according to the four different conditions. Segmentation was applied with respect to the occurrence of the stimuli (i.e., stimulus-locked). Automated artefact rejection procedures were applied after epoching: rejection criteria included a maximum voltage step of more than 50 μV/ms, a maximal value difference of 200 μV in a 200 ms interval or activity below 0.1 μV. Then the data was CSD-transformed (current source density transformation; Perrin et al., 1989) in order to eliminate the reference potential from the data. After the CSD-transformation, data were corrected relative to a baseline extending from 200 ms before stimulus presentation until stimulus onset and averaged. Based upon this stimulus-locking procedure, the N2 and P3 ERPs were quantified: The N2 was quantified at electrode FCz, which was the maximum of the N2 in the scalp topographies (cf. Fig. 3). The N2 was quantified relative to the pre-stimulus baseline and defined as the most negative peak occurring within the time interval of 250 till 320 ms. The P3 was quantified at electrode P1 and Pz according to the scalp topography (cf. Figs. 3 and 4). The P3 was defined as the most positive peak within a time range from 350 to 500 ms. Both components were quantified in amplitude and latency on single subject level.

Time–frequency decomposition (TF-decomposition)

Time–frequency (TF) analysis of stimulus-related potentials was performed by means of a continuous wavelet transform (CWT), applying Morlet wavelets (w) in the time domain to different frequencies (f):

$$w(t,f) = A\exp\left(-t^2/2\sigma_t^2\right)\exp(2i\pi ft),$$

t is time, $A = (\sigma_t\sqrt{\pi})^{-1/2}$, σ_t is the wavelet duration, and $i = \sqrt{-1}$. For analysis and TF-plots, a ratio of $f_0/\sigma_f = 5.5$ was used, where f_0 is the central frequency and σ_f is the width of the Gaussian shape in the frequency domain. The analysis was performed in the frequency range 0.5–20 Hz with a central frequency at 0.5 Hz intervals. For different

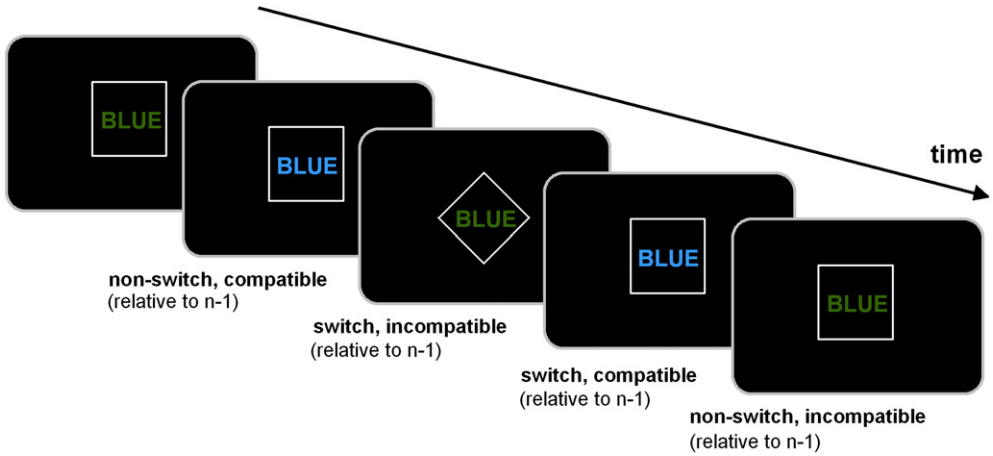

Fig. 1. Schematic diagram of the task conditions. A colour word, printed in different font colours is presented in the centre of the screen. The colour word is surrounded by a square or a rhomb denoting the rule in the current trial. Note that the gap of 150 ms between the cue and the target is not depicted in this figure. In relation to the previous trials (trial n − 1), the combination of colour word and surrounding square or rhomb allows four different conditions (please refer to the text for further details). (For interpretation of the references to color in this figure legend, the reader is referred to the web version of the article.)

f_0, time and frequency resolutions (or wavelet duration and spectral bandwidth; Tallon-Baudry et al., 1997) can be calculated as $2\sigma_t$ and $2\sigma_f$ respectively. σ_t and σ_f are related by the equation $\sigma_t = 1/(2\pi\sigma_f)$. For example, for $f_0 = 1$ Hz, $2\sigma_t = 1770$ ms and $2\sigma_f = 0.36$ Hz; for $f_0 = 3$ Hz, $2\sigma_t = 580$ ms and $2\sigma_f = 1.09$ Hz; for $f_0 = 5$ Hz, $2\sigma_t = 350$ ms and $2\sigma_f = 1.82$ Hz. The 'evoked wavelet power' was calculated, which refers to event-related changes in EEG power that are phase-locked with respect to the event onset across trials. The phase-synchronized oscillations in the EEG across trials were isolated by first time domain averaging the event-locked EEG epochs to derive the ERP. After this, the convolution with the complex wavelet was performed on this ERP average (Roach and Mathalon, 2008).

The segments used for the wavelet analysis were 4000 ms long; starting 2000 ms before stimulus onset and ending 2000 ms after stimulus onset. This epoch length was chosen to allow a reliable estimation of the evoked power of low frequent oscillations (e.g. Beste et al., 2010a; Ocklenburg et al., 2011). Maximal TF power and corresponding peak power latencies were measured in time intervals used for ERP quantification: i.e., N2 evoked wavelet power was estimated at the time point the N2 reached its maximum peak amplitude and the P3 evoked wavelet power was estimated at the time point the P3 amplitude in the time-domain analysis reached its maximum. Evoked wavelet power was quantified in the delta and theta frequency band. Their central frequencies were 3 and 5 Hz, so that the corresponding TF components covered roughly the delta (2.5–4 Hz) and theta (4–7 Hz) frequency bands (see: Beste et al., 2010a). The decomposition parameters used were the same for the N2 and P3 analysis. A time window from 600 to 800 ms prior to the response was used to estimate background noise. Wavelet power in the time range of interest was measured normalized to wavelet power at this baseline. Data quantification was performed on single subject level. TF power was $\log_{10}$-transformed to normalize the distributions for statistical analyses.

Source localisation (sLORETA analyses)

Source localisation was conducted using sLORETA (standardized low resolution brain electromagnetic tomography; Pascual-Marqui, 2002). sLORETA gives a single linear solution to the inverse problem based on extra-cranial measurements without a localisation bias (Marco-Pallares et al., 2005; Pascual-Marqui, 2002; Sekihara et al., 2005). sLORETA has been validated in simultaneous EEG/fMRI studies (Vitacco et al., 2002). For sLORETA, the intracerebral volume is partitioned in 6239 voxels at 5 mm spatial resolution and the standardised current density at each voxel is calculated in a realistic head model (Fuchs et al., 2002) using the MNI152 template (Mazziotta et al., 2001). In the present study the voxel-based sLORETA-images were compared between groups using the sLORETA-built-in voxel-wise randomisation tests with 5000 permutations, based on statistical non-parametric mapping. Voxels with significant differences ($p<.05$, corrected for multiple comparisons) between groups were located in the MNI-brain and Brodman areas (BAs) as well as coordinates in the MNI-brain were determined using the sLORETA software (www.unizh.ch/keyinst/NewLORETA/sLORETA/sLORETA.htm). The comparison of sLORETA images between groups (controls vs. pre-HDs) was based on the original ERPs in the time domain on the basis of scalp voltages. sLORETA was applied on the N2 and P3 ERP data.

MRI scanning and analyses

Structural MRI scanning was conducted to assess caudate head volume. Scanning data was available for N = 27 pre-HDs (3 pre-HDs had to be excluded). MR-imaging was performed on a 1.5 T scanner (Magnetom SymphonyTM, Siemens, Erlangen, Germany) using a standard head coil and a Turbo FLASH 3D sequence with the following parameters: TE (echo time): 3.93 ms, TR (repetition time): 1900 ms, TI (inversion time): 1100 ms, FA: 15°, NA: 1, resolution: 1 mm × 1 mm, 128 sagittal slices, voxel-size in slice selected direction 1.0 mm. Subjects were positioned within the head coil using a standard procedure according to outer anatomical markers. Caudate volume was calculated using the manual tracing method described by Aylward et al. (2004). To correct for inter-individual variations due to gender and head size, all caudate head volumes were normalised against the total intracranial volume (TIV) (e.g. Whitwell et al., 2001), by calculating the ratio between TIV and caudate head volume. Both of these measures, i.e. the uncorrected caudate volume (Aylward et al., 2004) and the caudate head volume corrected for TIV were used in regression analyses with the electrophysiological parameters.

Statistical analyses

Data (RTs, error rates, ERP amplitudes and latencies, ERP power) was analysed using mixed and univariate analysis of variance (ANOVAs). In the mixed ANOVAs, the factors "trial type (switch vs. non-switch)" and "compatibility (compatible vs. incompatible)" were within-subject factors. The factor "group (pre-HD vs. controls)" was used as between-subject factor. Based on scalp topography of the ERPs, an additional within-subject factor "electrode" was included, if necessary. When appropriate, the degrees of freedom were adjusted using Greenhouse–Geisser correction. All post-hoc tests were Bonferroni-corrected. Kolmogorov–Smirnov tests revealed that all relevant variables were normally distributed (all $z<0.5$; $p>.4$; one-tailed). As a measure of variability the standard error of the mean (SEM) is given.

Results

Behavioural data

The response times (RTs) were analysed in a mixed effects ANOVA using "trial type (switch vs. non-switch)" and "compatibility (compatible vs. incompatible)" as within-subject factors. "Group" (pre-HDs vs. controls) served as between-subject factor. The main effect "compatibility" revealed that RTs were longer on incompatible (735 ± 7) than on compatible trials (628 ± 5) ($F(1,58) = 379.88$; $p<.001$; $\eta^2 = .86$). The main effect "switching" revealed that RTs were longer on switch trials (726 ± 5) than on repeat trials (637 ± 5) ($F(1,58) = 247.85$; $p<.001$; $\eta^2 = .81$). The main effect "group" ($F(1,58) = 9.91$; $p = .003$; $\eta^2 = .14$) revealed that RTs were longer in pre-HDs (689 ± 4) than in controls (664 ± 5). The ANOVA revealed an interaction "trial type × compatibility × group" ($F(1,58) = 11.64$; $p = .001$; $\eta^2 = .16$). This interaction is plotted in Fig. 2.

Bonferroni-corrected independent samples t-tests indicate that the groups did not differ in their RTs on compatible switch and non-switch trials, as well as on incompatible non-switch trials ($t(58) < -0.95$; $p>.2$). However, they differed on incompatible switch trials ($t(58) = 6.11$; $p<.001$), where RTs were much longer for the pre-HD (834 ± 10) than for the control group (765 ± 9).

The analysis of error rates revealed that error rates were higher on incompatible (14.6 ± 0.2), than on compatible trials (12.5 ± 0.3) ($F(1,58) = 37.41$; $p<.001$; $\eta^2 = .39$), as well as on switch trials (14.5 ± 0.3) compared to non-switch trials (12.7 ± 0.2) ($F(1,58) = 18.59$; $p<.001$; $\eta^2 = .24$). There was no group difference and also all other main or interaction effects were not significant (all $F<0.9$; $p>.3$).

Switch costs (behaviour)

Switch costs were calculated by subtracting mean RTs on non-switch trials from mean RTs on switch trials. Switch costs were higher in the incompatible (129 ± 8) than in the compatible condition (49 ± 6) ($F(1,58) = 59.44$; $p<.001$; $\eta^2 = .50$) and also higher in pre-HDs (110 ± 8) than in controls (68 ± 7) ($F(1,58) = 13.82$; $p<.001$; $\eta^2 = .19$). However, there was an interaction "group × compatibility"

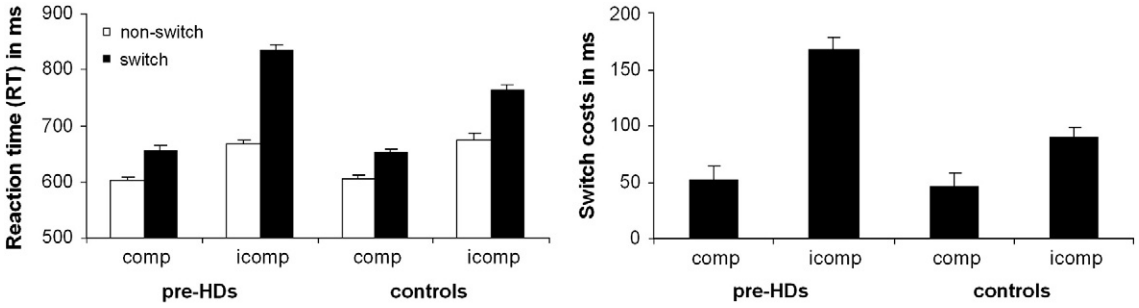

Fig. 2. Left side: mean reaction time (RT) in milliseconds (±SEM) for compatible and incompatible switch and non-switch trials, separated for pre-HDs and controls. Right side: mean switch costs (RTs) (±SEM) for the compatible and incompatible condition for pre-HDs and controls.

($F(1,58)=11.64$; $p<.001$; $\eta^2=.16$). Post-hoc tests revealed that group differences in switch costs were only evident in the incompatible condition ($t(58)=5.7$; $p<.001$), but not in the compatible condition ($t(58)=0.39$; $p>.4$). Concerning error rates, there were no differences in switch costs between groups (all $F<0.9$; $p>.3$).

Neurophysiological data

N2 data

The N2 is shown in Fig. 3A. The N2 showed a clear maximum at FCz. The N2 at FCz was analysed in a mixed ANOVA using "task" and "compatibility" as within-subject factors; "group" served as between-subject factor. The N2 was larger (i.e., more negative) on incompatible (-5.8 ± 0.1), than on compatible trials (-4.2 ± 0.1) ($F(1,58)=123.66$; $p<.001$; $\eta^2=.68$), as well as on switch (-5.9 ± 0.1) than on non-switch trials (-4.1 ± 0.2) ($F(1,58)=258.12$; $p<.001$; $\eta^2=.81$). The N2 was attenuated in pre-HDs (-4.7 ± 0.2), compared to controls (5.3 ± 0.2) ($F(1,58)=44.19$; $p<.001$; $\eta^2=.43$). An interaction "compatibility × trial type × group" ($F(1,58)=18.65$; $p<.001$; $\eta^2=.24$) was found. This interaction is given in Fig. 3B.

To explore this interaction further independent samples t-tests, serving as post-hoc tests were run. These tests revealed that the groups did not differ in their N2 amplitudes on compatible ($t(58)=-0.13$; $p>.4$) and incompatible non-switch trials ($t(58)=-0.65$; $p>.3$) as well as on compatible switch trials ($t(58)=-0.94$; $p>.2$). However, on incompatible switch trials the N2 amplitude was attenuated in pre-HDs (-5.5 ± 0.3) compared to controls (-7.6 ± 0.2) ($t(58)=-7.2$; $p<.001$). Paired samples t-tests within each group revealed that the N2 amplitude increased in controls from the compatible to the incompatible switching condition ($t(29)=-7.61$; $p<.001$), while in pre-HDs, no changes in N2 amplitude were evident ($t(29)=-1.1$; $p>.15$). As to the latencies, there was no interaction "compatibility × trial type × group" ($F(1,58)=0.5$; $p>.3$). The sLORETA analyses on the N2 ERP suggest that group differences in incompatible switch trials were related to regions in the rostral cingulate zone, encompassing BA6 and BA8, centered in BA24 and BA23.

P3 data

The P3 is shown in Fig. 4A. It showed a parietal maximum (Pz) with strong left displacement (P1). Therefore it was analysed at both electrodes. The P3 was analysed in a mixed ANOVA using "electrode (P1, Pz)", "compatibility" and "task" as within-subject factors and "group" as between-subject factor.

The P3 was larger at electrode Pz (21.8 ± 0.3), compared to P1 (19.9 ± 0.2) ($F(1,58)=58.32$; $p<.001$; $\eta^2=.50$). The P3 was also larger for compatible (21.5 ± 0.2), than for incompatible trials (20.3 ± 0.3) ($F(1,58)=53.38$; $p<.001$; $\eta^2=.47$); and for non-switch trials (21.8 ± 0.2), compared to switch trials (20 ± 0.1) ($F(1,58)=90.30$; $p<.001$; $\eta^2=.60$). There was no difference in P3 amplitudes between pre-HDs and controls ($F(1,58)=0.46$; $p>.4$). However, there was an interaction "electrode × compatibility × task × group" ($F(1,58)=7.53$; $p=.008$; $\eta^2=.12$). Subsequent mixed ANOVAs for electrode P1 and Pz separately revealed that an interaction "compatibility × trial type × group" was evident for electrode Pz ($F(1,58)=7.34$; $p<.001$; $\eta^2=.11$), but not for electrode P1 ($F(1,58)=0.89$; $p>.3$). Therefore, only electrode Pz was analysed further. The interaction for electrode Pz is given in Fig. 3B. For electrode Pz it is shown that the P3 amplitude did not differ between groups on compatible trials ($t(58)=-0.49$; $p>.3$; pre-HDs: 25.02 ± 0.37, controls: 25.14 ± 0.45) and incompatible non-switch trials ($t(58)=-0.05$; $p>.6$; pre-HDs: 22.73 ± 0.42; controls: 22.61 ± 0.41) and on compatible switch trials ($t(58)=0.24$; $p>.5$; pre-HDs: 21.56 ± 0.54, controls: 21.48 ± 0.43), but on incompatible switch trials ($t(58)=-3.01$; $p=.004$; pre-HDs: 17.29 ± 0.33, controls: 19.39 ± 0.67). On incompatible switch trials, the P3 was larger for the pre-HDs (19.3 ± 0.6), compared to controls (17.1 ± 0.4). The sLORETA analyses on the P3 ERPs suggest that group differences in incompatible switch trials were related to regions in the parietal lobe, encompassing BA5 and BA7, centered in BA7.

The latencies of the P3 were also analysed at electrode Pz and revealed an interaction "compatibility × trial type × group" ($F(1,58)=9.32$; $p=.003$; $\eta^2=.13$). Similar to the amplitudes, post-hoc tests revealed that the groups did not differ in their P3 latencies on compatible ($t(58)=0.26$; $p>.4$) and incompatible non-switch trials ($t(58)=0.12$; $p>.3$) as well as on compatible switch trials ($t(58)=-0.41$; $p>.3$). Yet, on incompatible switch trials the P3 latency was longer in pre-HDs (425 ± 5), compared to controls (397 ± 5) ($t(58)=7.9$; $p<.001$), which parallels the prolongation of RTs in this condition. As to the main effects, the latencies were longer on incompatible (388 ± 5) than on compatible trials (336 ± 4) ($F(1,58)=376.28$; $p<.001$; $\eta^2=.86$) and on switch (385 ± 3) than on non-switch trials (337 ± 5) ($F(1,58)=371.45$; $p<.001$; $\eta^2=.86$). P3 latencies were also longer for pre-HDs (365 ± 2) than for controls (358 ± 3) ($F(1,58)=6.13$; $p=.016$; $\eta^2=.09$).

Switch costs (N2 and P3 data)

Switch costs reflected in latencies and amplitudes were calculated by subtracting parameters from non-switch trials from parameters derived from switch trials. For all parameters (i.e., N2 amplitudes and latencies, P3 amplitudes and latencies), there was an interaction "compatibility × group" ($F(1,58)>9.32$; $p<.003$; $\eta^2>.13$). Bonferroni-corrected post hoc tests revealed that group differences in switching costs were solely evident in the incompatible condition. The difference in N2 amplitudes was larger in controls (-2.1 ± 0.2) than in pre-HDs (-0.5 ± 0.2) ($t(58)=-5.17$; $p<.001$). The difference in P3 amplitudes ($t(58)=-3.43$; $p=.001$) and latencies ($t(58)=4.30$; $p<.001$) was also larger for controls (amplitudes: -5.4 ± 0.3; latencies: 60 ± 5) than for pre-HDs (amplitudes: -3.2 ± 0.3; latencies: 33 ± 5).

Time–frequency analyses (TF-analyses)

The ERP analyses suggest that the N2 was decreased in its amplitude and the P3 was increased in its amplitude in pre-manifest

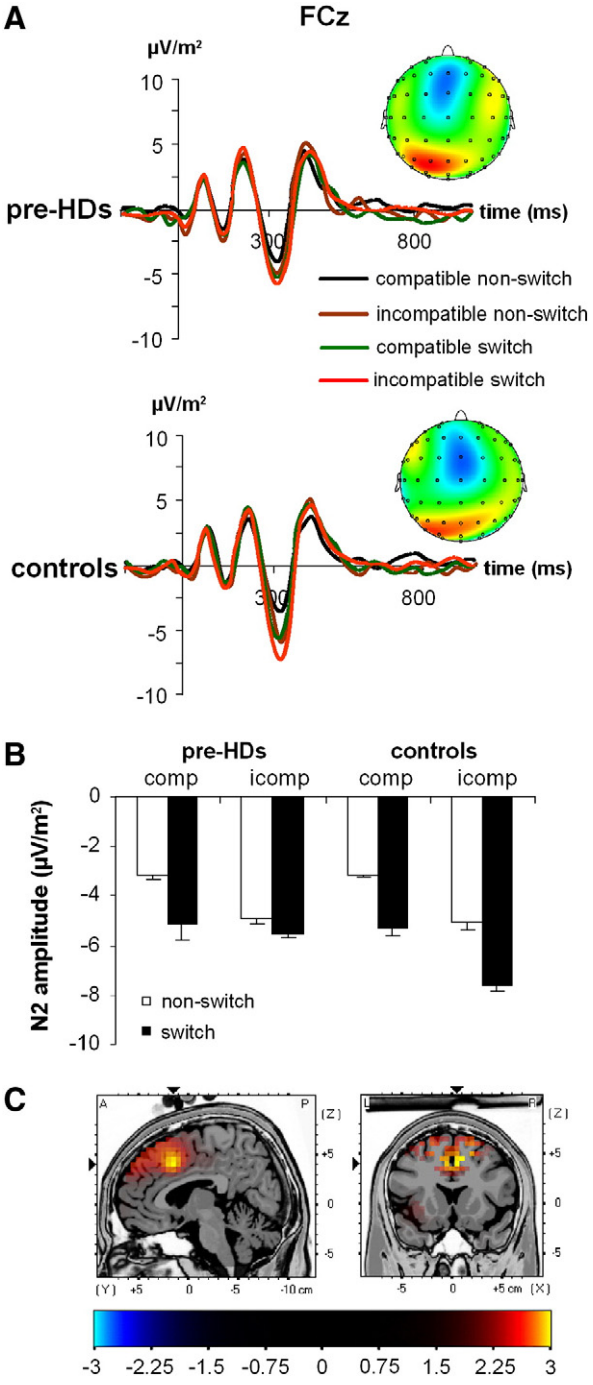

Fig. 3. (A) Stimulus-locked ERP at electrode FCz for compatible and incompatible switch and non-switch trials. The pre-HD and control groups are given separately. A representative scalp topography map is given for pre-HDs and controls at the time point of the peak of the N2. Time point 0 denotes the time point of stimulus delivery. (B) Histogram of the mean N2 amplitude ($\mu V/m^2$) ($\pm$SEM) in the different conditions. (C) sLORETA sources of the N2 ERP.

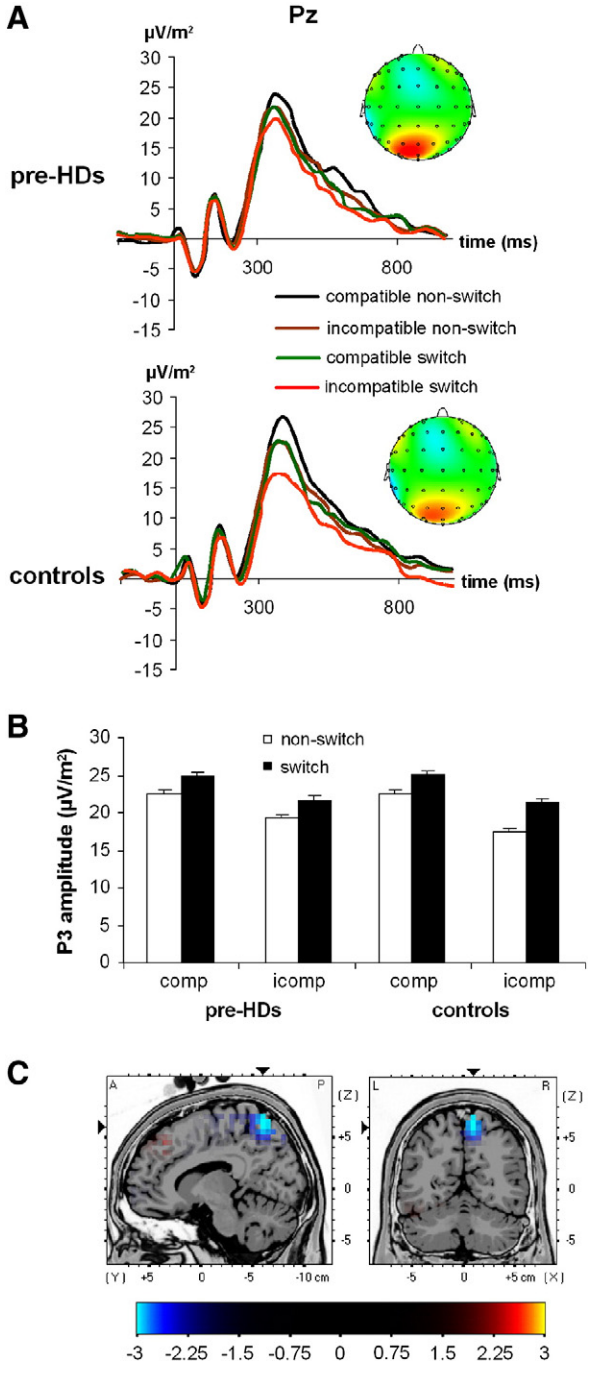

Fig. 4. (A) Stimulus-locked ERP at electrode Pz for compatible and incompatible switch and non-switch trials. The pre-HD and control groups are given separately. A representative scalp topography map is given for pre-HDs and controls at the time point of the peak of the P3. Time point 0 denotes the time point of stimulus delivery. (B) Histogram of the mean P3 amplitude ($\mu V/m^2$) ($\pm$SEM) in the different conditions. (C) sLORETA sources of the P3 ERP.

Huntington's disease gene mutation carriers (pre-HDs), especially when switching processes had to be executed on incompatible (i.e., Stroop-related) stimulus material. Using time–frequency (TF) analyses, we further examined evoked wavelet power in the delta and theta frequency range to complement the time-domain analyses. We focussed on the incompatible switch trials, as only this condition revealed differences between the groups. TF-analyses were performed for electrode FCz for the N2-range and electrode Pz for P3-range.

N2 effects

For the delta frequency band (at 3 Hz), we found a "compatibility × trial type × group" interaction ($F(1,58) = 38.25$; $p < .001$; $\eta^2 = .39$). Bonferroni-corrected post-hoc test (independent samples t-tests) showed that the groups did not differ on compatible and incompatible non-switch trials and on compatible switch trials (all $t(58)s < 1.5$; $p > .2$). On incompatible switch trials, the groups differed with the pre-HD group showing lower delta frequency evoked power (3.48 ± 0.04), than the control group (3.61 ± 0.03) ($t(58) = -23.39$;

$p<.001$). Controls revealed an increase in evoked wavelet power from the compatible switching to the incompatible switching condition ($t(29)=-6.92$; $p<.001$). In pre-HDs, there was no increase in evoked wavelet power between these conditions ($t(29)<0.8$; $p>.3$). These results are depicted in Fig. 5A. When using the theta frequency band (5 Hz) no interaction effects modulated by the factor group were evident (Fs 0.6; $p>.4$).

P3 effects

Comparable to the N2 analysis, there was an interaction "compatibility × trial type × group", too ($F(1,58)=5.60$; $p=.021$; $\eta^2=.08$) (Fig. 5B). Post-hoc tests showed that the groups did not differ on compatible and incompatible non-switch trials, as well as on compatible switch trials ($t(58)s<1.41$; $p>.2$). Yet, on incompatible switch trials the pre-HD group revealed a higher evoked delta band power (3.6 ± 0.1), than the control group (3.47 ± 0.03) ($t(58)=14.06$; $p<.001$). These results parallel the findings obtained from the time domain analyses.

An implicit assumption of a frequency power analysis is that power density in the pre-stimulus (baseline) period reflects the background non-event related EEG rhythms, which may be critical with respect to the relatively short interval between stimulus and response. Therefore, we quantified the power at baseline (i.e., we computed the mean TF-power in the time interval resembling the baseline) and included it as a covariate in the ANOVAs. This procedure (i.e., the inclusion of baseline TF power) did not change the pattern of results (all covariate $Fs<0.4$; $p>.5$). Hence, we assume that the results are unbiased with respect to baseline activity.

Correlational analyses

The above analyses show that group-dependent modulations in the N2 and P3 phase-locking are mediated via distinct brain areas. In a last step, we analysed how modulations in N2 and P3 phase-locking are related to clinically relevant parameters. The strength of the individuals evoked power in the N2 range on incompatible switch trials was inversely related to the DBS ($r=-.558$; $R^2=.30$; $p<.001$) and related to the YTO according to Ranen et al. (1995) ($r=.782$; $R^2=.61$; $p=.001$) and Langbehn et al. (2004) ($r=.600$; $R^2=.36$; $p=.001$), the probability of eAO within the next five years ($r=.648$; $R^2=.40$; $p<.001$). These correlations suggest that N2-related processes become more compromised the close the estimated onset of disease manifestation and the higher the genetic disease load. Additional regression analyses showed that the amount of N2 evoked power was related to caudate head volume ($r=.426$; $R^2=.17$; $p=.012$), also when corrected using total intra-cranial volume (TIV) ($r=-.454$; $R^2=.20$; $p=.009$). The results show that N2 evoked power, when caudate volume was smaller. As to the P3 on incompatible switch trials, there was no correlation of evoked wavelet power with any of these parameters ($r<.061$; $p>.15$). Scatterplots for the correlational analyses regarding N2 evoked power are given in Fig. 6.

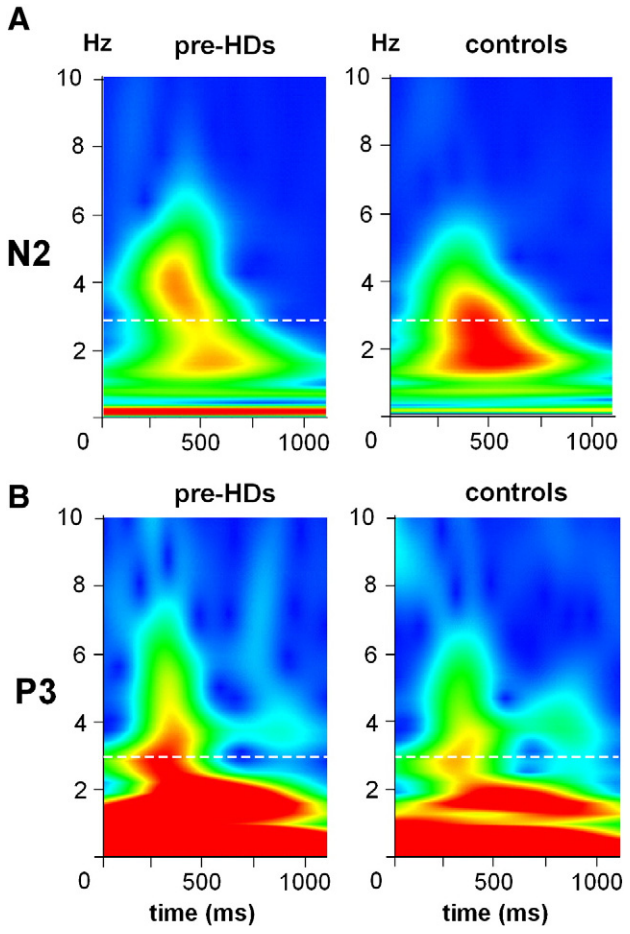

Fig. 5. (A) Time–frequency plot for electrode FCz (N2 evoked power) in incompatible switching condition for pre-HDs and controls. The ordinate denotes the frequency; the abscissa the time in milliseconds (ms). The power of the different frequency bands is colour-coded. Time point 0 denotes the time point of stimulus delivery. The dotted white lines denote the frequency of 3 Hz. (B) Time–frequency plot for electrode Pz (P3 evoked power) in incompatible switching condition for pre-HDs and controls.

Discussion

In the current study, we investigated the role of fronto-striatal loops for the parallel execution of flexible response adaptation and conflict monitoring in a combined Stroop-Task-Switching paradigm. Recent neurocomputational models of fronto-striatal circuit functioning (Frank, 2005; Humphries et al., 2006; Leblois et al., 2006; Redgrave et al., 1999) imply that parallel processing in these loops is only possible to a certain extend, which depends on the ability to represent different action representations in MSN ensembles. Examining the above, we inferred neurophysiological mechanisms from ERPs as well as evoked EEG oscillations (e.g. Basar et al., 2001) in a major basal ganglia disorder (i.e., pre-manifest Huntington's disease gene mutation carriers; pre-HDs). Neurophysiological data was integrated with structural MRI volumetric data and source localisation using sLORETA was carried out. Pre-manifest Huntington's disease gene mutation carriers were examined because changes in MSNs are a characteristic of this disease (e.g. Cepeda et al., 2007; Thomas et al., 2011) and already evident in the pre-manifest stage (Tabrizi et al., 2009).

The results show that pre-HDs revealed higher switch costs when task-switching and the resolution of conflict occurred in parallel: when one switched from word reading to colour naming ("switch incompatible" in the current study), the switch costs are greater in pre-HDs than in controls. When one switched from colour naming to word reading ("switch compatible" in the current study) switch costs were generally lower and also not different between the groups. In the other conditions, where high demands on conflict monitoring did not co-incide with task-switching, no group differences were evident. The observed effect on compatible and incompatible switch trials may be regarded at odds with the 'asymmetric switch cost effect' usually reported in such paradigms (e.g. Allport et al., 1994; Schneider and Anderson, 2010). However, it has to be noted that such asymmetric switch cost effects disappear, when a gap between cue (rhomb or square) and the target stimulus is evident (see: Monsell et al., 2000), as it was the case in our study. The behavioural data shows that a neurodegenerative processes in fronto-striatal loops, as evident in pre-HDs, primarily compromise flexible adaptation of actions, when this process co-incides with high demands on

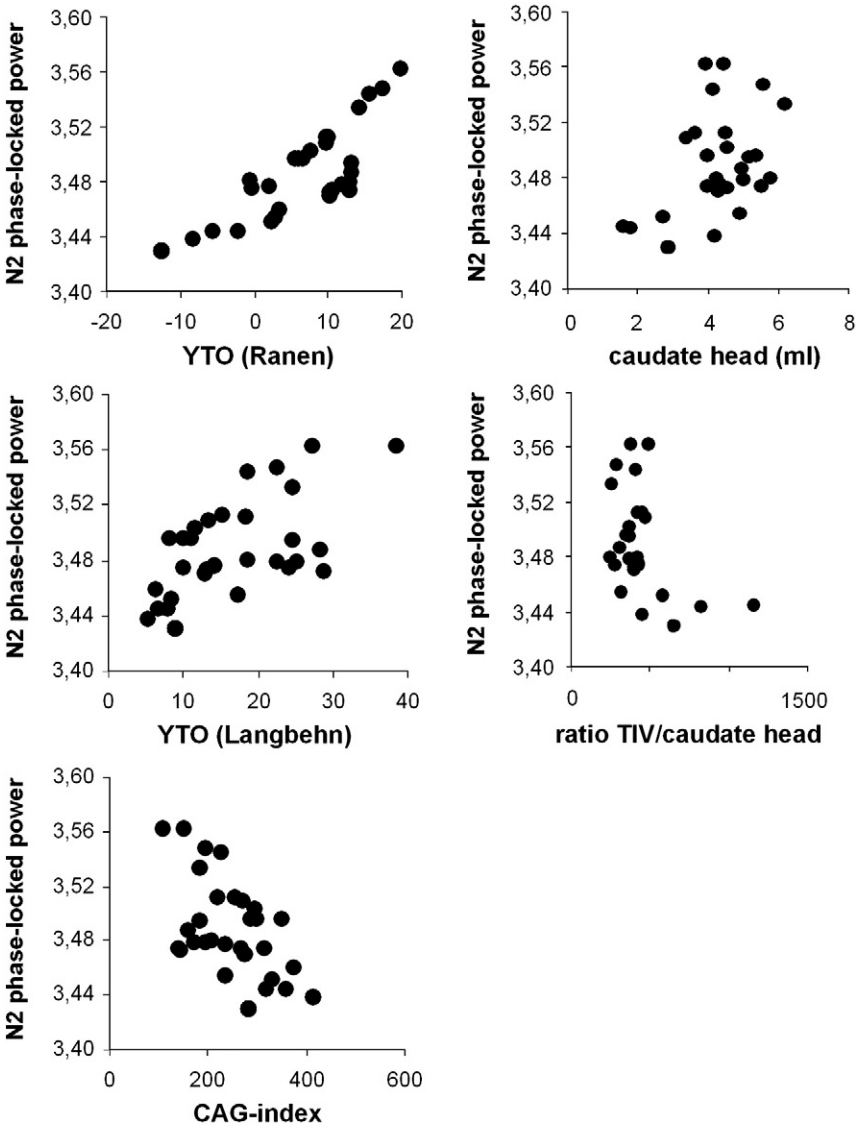

Fig. 6. Scatterplots denoting the correlation between N2 evoked wavelet power and the years until estimated age of onset (YTO) according Ranen et al. (1995) (top), Langbehn et al. (2004) (middle) and the 'disease burden score' (bottom) are depicted at the left side of the panel. Scatterplots denoting the correlation between N2 evoked wavelet power and corrected and non-corrected caudate head volume are presented on the right side of the panel.

conflict monitoring. When conflict monitoring and flexible response adaptation do not co-incide, a high integrity of fronto-striatal loops seems to be dispensable.

The neurophysiological data underlines the pattern found within our behavioural data and further suggest that this pattern of results is due to a differential affection of conflict monitoring and working memory processes:

With respect to conflict monitoring processes, the N2 (e.g. Folstein and van Petten, 2008; van Veen and Carter, 2002) group differences were only evident on incompatible switch trials which completely underlines the behavioural data. The N2 was attenuated in pre-HDs. Also, evoked wavelet power in the delta frequency band within the N2 time range was lower, when compared to controls. Modulations in the delta frequency band have previously been shown to reflect processes related to the inhibition of responses (Ocklenburg et al., 2011). The data may thus reflect an inability to suppress the irrelevant, previous task-set (e.g. Mayr, 2001) and select the appropriate response (Gajewski et al., 2010), when fronto-striatal loops are compromised. The sLORETA analyses on ERPs suggest that functional changes in the anterior cingulate (BA32 and BA24) may mediate the above pattern reflected by the N2. The sources obtained for the N2 ERP are in accordance with other studies (e.g. Folstein and Van Petten, 2008; van Veen and Carter, 2002). In conditions of high conflict, additional response selection processes necessary to adjust behaviour due to the changed task rule may overstrain fronto-striatal circuits. This interpretation is underlined by the fact that controls revealed an increase in N2 amplitudes (e.g. Jackson et al., 2001; Karayanidis et al., 2003) and N2 evoked wavelet power in conditions with high conflict, while pre-HDs did not intensify N2-related processes. The lack of intensification of processes reflected by the N2 has previously been shown to be related to higher switch costs (Gajewski et al., 2010).

With respect to working memory processes P3 parameters are important. The prolongation of P3 latency, reductions of P3 amplitude and evoked wavelet power, as observed in pre-HDs, have been suggested to reflected increased working memory load (e.g. Kok, 2001), or modulations in attentional set shifting (e.g. Neuhaus et al., 2011). Alterations in the P3 have been observed in several other studies examining Huntington's disease (e.g. Beste et al., 2008a,b,c, 2010b; Münte et al., 1997), yet mostly in more severe disease stages. Deficits in working memory processes related to the updating, organisation and implementation of the new task-set (e.g. Barcelo et al., 2006; Gehring et al.,

2003; Goffaux et al., 2006; Karayanidis et al., 2003; Nicholson et al., 2005, 2006; Rushworth et al., 2002) during task switching only occurred in situations requiring parallel conflict monitoring and flexible response adaptation processes. Source localisation analyses on ERPs suggest that functional changes underlying these working memory deficits are related to the superior parietal cortex (BA7). This is well in line with studies stressing the importance of parietal areas for working memory and task switching processes (e.g. Gottlieb, 2007; Hedden and Gabrieli, 2010; Jamadar et al., 2010).

Possible neuronal mechanisms and implications

The above results suggest that processes related to conflict monitoring and working memory are affected in pre-HDs during parallel processing. However, the effect in working memory processes was lower than the effect observed for conflict resolution processes (N2 effects). This suggests that deficits observed in conflict monitoring are the driving factor in difficulties related to the parallel execution of flexible response adaptation and conflict monitoring. With respect to the sLORETA results on ERPs, N2-related processes (conflict monitoring) are related to the ACC, while P3-related processes (working memory) were related to parietal areas. MRI volumetric caudate head volume predicted modulation of conflict monitoring (N2 data), but not of working memory processes (P3 data). In contrast to the ACC, parietal areas are not directly embedded in fronto-striatal loops (e.g. Chudasama and Robbins, 2006). In the pre-manifest disease stage, neurodegenerative effects on MSNs are already evident (e.g. Cepeda et al., 2007) and highly genetically determined (Thomas et al., 2011). It is possible that dysfunctions observed for the ACC in the sLORETA N2 ERP results reflect an indirect effect of dysfunctions at the striatal level. Clearly, MSN functioning cannot be directly examined using MRI volumetric measurement, which accounts for structural effects on a macroscopic level. However, it has been shown that especially MSNs are affected in HD (e.g. Cepeda et al., 2007) and vulnerable to mutant huntingtin (Thomas et al., 2011). The DBS gives an estimate of the amount of the individual's mutant huntingtin exposure (Tabrizi et al., 2009). A higher DBS was related to higher switch costs and an attenuated N2. Therefore, it is possible that a dysfunction and degeneration of MSNs may affect processing of the ACC as the cortical endpoint of this functional basal ganglia loop.

The results have implications for models stating that MSNs play a crucial role in action selection within fronto-striatal loops (Gurney et al., 2004) and that these mechanisms are governed by a winner-takes-all network (WTA) (Bar-Gad et al., 2003; Plenz, 2003). Within such a network, parallel processing is theoretically possible to some extend (Redgrave et al., 1999), depending on the ability to represent different action representations at the same time in fronto-striatal networks and especially MSN ensembles. The above discussion on the N2-effects suggests that pre-HDs are not able to intensify N2-related processes, reflecting an inability to process additional response selection demands, necessary to adjust behaviour and to inhibit the previous task-set. It is possible that striatal structures in pre-HDs are not able to represent more than one process at once, leading to deficits, when two processes impinge upon striatal structures. Besides structural changes in the MSN network, deficits in dopaminergic neural transmission, which are evident in pre-HDs (e.g. van Oostrom et al., 2009) and modulate MSN functioning (Surmeier et al., 2007).

Summary

In summary, the results reveal neuronal (electrophysiological) mechanisms that mediate parallel conflict monitoring processes and flexible adaptation of actions. While both, response monitoring and working memory processes, seem to play a role, especially response selection processes and ACC–basal ganglia networks seem to be the driving force in mediating parallel conflict monitoring and flexible adaptation of actions. This is corroborated using source localisation of ERP data by means of sLORETA. The time–frequency data shows that differences in the integrity of fronto-striatal loops predominantly affect the delta frequency band. MRI volumetric measurements and estimators for neurobiological processes compromising MSN function, also underline the importance of ACC–basal ganglia networks. From a neurological point of view, the results suggest that situations requiring a parallel execution of fronto-striatal loop processes are sensitive to early changes in cognitive processes in Huntington's disease. From a broader neurobiological perspective, the results suggest compromised fronto-striatal loops may not be able to represent different kinds of information in parallel and may therefore not be able to perform parallel processing of different cognitive functions.

Acknowledgments

This research was supported by a grant from CHDI foundation to C.B. and C.S. and by a DFG grant BE 4045/10-1 to C.B. We thank all participants. We thank the unknown reviewers for their constructive comments on the manuscript.

References

Allport, A., Styles, E.A., Hsieh, S., 1994. Shifting intentional set: exploring the dynamic control of tasks. In: Umilta, C., Moscovitch, M. (Eds.), Attention and Performance: XV. Erlbaum, Hillsdale (NJ), pp. 421–452.
Aron, A.R., Watkins, L., Sahakian, B.J., Monsell, S., Barker, R.A., Robbins, T.W., 2003. Task-set switching deficits in early-stage Huntington's disease: implications for basal ganglia function. J. Cogn. Neurosci. 15, 629–642.
Aylward, E.H., Sparks, B.F., Field, K.M., Yallapragada, V., Shpritz, B.D., Rosenblatt, A., Brand, J., Gourley, L.M., Liang, K., Zhou, H., Margolis, R.L., Ross, C.A., 2004. Onset and rate of striatal atrophy in preclinical Huntington disease. Neurology 63, 66–72.
Barcelo, F., Escera, C., Corral, M.J., Perianez, J.A., 2006. Task switching and novelty processing activate a common neural network for cognitive control. J. Cogn. Neurosci. 18, 1734–1748.
Bar-Gad, I., Morris, G., Bergman, H., 2003. Information processing, dimensionality reduction and reinforcement learning in the basal ganglia. Prog. Neurobiol. 71, 439–473.
Basar, E., Schürmann, M., Demiralp, T., Basar-Eroglu, C., Ademoglu, A., 2001. Event-related oscillations are 'real brain responses' — wavelet analysis and new strategies. Int. J. Psychophysiol. 39, 91–127.
Beste, C., Saft, C., Yordanova, J., Andrich, J., Gold, R., Falkenstein, M., Kolev, V., 2007. Functional compensation or pathology in cortico-subcortical interactions in pre-clinical Huntington's disease? Neuropsychologia 45, 2922–2930.
Beste, C., Saft, C., Andrich, J., Gold, R., Falkenstein, M., 2008a. Stimulus–response compatibility in Huntington's disease: a cognitive-neurophysiological analysis. J. Neurophysiol. 99, 1213–1223.
Beste, C., Saft, C., Güntürkün, O., Falkenstein, M., 2008b. Increased cognitive functioning in symptomatic Huntington's disease as revealed by behavioral and event-related potential indices of auditory sensory memory and attention. J. Neurosci. 28, 11695–11702.
Beste, C., Saft, C., Andrich, J., Gold, R., Falkenstein, M., 2008c. Response inhibition in Huntington's disease — a study using ERPs and sLORETA. Neuropsychologia 46, 1290–1297.
Beste, C., Kolev, V., Yordanova, J., Domschke, K., Falkenstein, M., Baune, B.T., Konrad, C., 2010a. The role of the BDNF Val66Met polymorphism for the synchronization of error-specific neural networks. J. Neurosci. 30, 10727–10733.
Beste, C., Willemssen, R., Saft, C., Falkenstein, M., 2010b. Response inhibition subprocesses and dopaminergic pathways: basal ganglia disease effects. Neuropsychologia 48, 366–373.
Beste, C., Baune, B.T., Domschke, K., Falkenstein, M., Konrad, C., 2010c. Dissociable influences of NR2B-receptor related neural transmission on functions of distinct associative basal ganglia circuits. Neuroimage 52, 309–351.
Botvinick, M.M., Cohen, J.D., Carter, C.S., 2004. Conflict monitoring and anterior cingulate cortex: an update. Trends Cogn. Sci. 8, 539–546.
Cepeda, C., Wu, N., Andre, V.M., Cummings, D.M., Levine, M.S., 2007. The corticostriatal pathway in Huntington's disease. Prog. Neurobiol. 81, 253–271.
Chudasama, Y., Robbins, T.W., 2006. Functions of fronto-striatal systems in cognition: comparative neuropsychopharmacological studies in rats, monkeys and humans. Biol. Psychol. 73, 19–38.
Eppinger, B., Kray, J., Mecklinger, A., John, O., 2007. Age differences in task switching and response monitoring: evidence from ERPs. Biol. Psychol. 75, 52–67.
Folstein, J.R., Van Petten, C., 2008. Influence of cognitive control and mismatch on the N2 component of the ERP: a review. Psychophysiology 45, 152–170.
Frank, M.J., 2005. Dynamic dopamine modulation in the basal ganglia: a neuro-computational account of cognitive deficits in medicated and non-medicated Parkinsonism. J. Cogn. Neurosci. 17, 51–72.
Fuchs, M., Kastner, J., Wagner, M., Hawes, S., Ebersole, J.S., 2002. A standardized boundary element method volume conductor model. Clin. Neurophysiol. 113, 702–712.

Gajewski, P.D., Kleinsorge, T., Falkenstein, M., 2010. Electrophysiological correlates of residual switch costs. Cortex 46, 1138–1148.
Gehring, W.J., Bryck, R.L., Jonides, J., Albin, R.L., Badre, D., 2003. The mind's eye, looking inward? In search of executive control in internal attention shifting. Psychophysiology 40, 572–585.
Goffaux, P., Phillips, N.A., Sinai, M., Pushkar, D., 2006. Behavioral and electrophysiological measures of task switching during single and mixed-task conditions. Biol. Psychol. 72, 278–290.
Gottlieb, J., 2007. From thought to action: the parietal cortex as a bridge between perception, action, and cognition. Neuron 53, 9–16.
Gurney, K., Prescott, T.J., Wickens, J.R., Redgrave, P., 2004. Computational models of the basal ganglia: from robots to membranes. Trends Neurosci. 27, 453–459.
Hanslmayr, S., Pastötter, B., Bäuml, K.-H., Gruber, S., Wimber, M., Klimesch, W., 2008. The electrophysiological dynamics of interference during the Stroop task. J. Cogn. Neurosci. 20, 215–225.
Hedden, T., Gabrieli, J.D., 2010. Shared and selective neural correlates of inhibition, facilitation, and shifting processes during executive control. Neuroimage 51, 421–431.
Humphries, M.D., Stewart, R.D., Gurney, K.N., 2006. A physiological plausible model of action selection and oscillatory activity in the basal ganglia. J. Neurosci. 26, 12921–12942.
Huntington Study Group, 1996. Unified Huntington's disease rating scale: reliability and consistency. Mov. Disord. 11, 136–142.
Jackson, G.M., Swainson, R., Cunnington, R., Jackson, S.R., 2001. ERP correlates of executive control during repeated language switching. Biling. Lang. Cogn. 4, 169–178.
Jamadar, S., Hughes, M., Fulham, W.R., Michie, P.T., Karayanidis, F., 2010. The spatial and temporal dynamics of anticipatory preparation and response inhibition in task-switching. Neuroimage 51, 432–449.
Jung, E.Y., Shim, I., 2011. Differential DAergic control of D1 and D2 receptor agonist over locomotr activity and GABA level in the striatum. Exp. Neurobiol. 20, 153–157.
Karayanidis, F., Coltheart, M., Michie, P.T., Murphy, K., 2003. Electrophysiological correlates of anticipatory and poststimulus components of task switching. Psychophysiology 40, 329–348.
Kassubek, J., Juengling, F.D., Ecker, D., Landwehrmeyer, G.B., 2005. Thalamic atrophy in Huntington's disease co-varies with cognitive performance: a morphometric MRI analysis. Cereb. Cortex 15, 846–853.
Kehagia, A.A., Cools, R., Barker, R., Robbins, T.W., 2009. Switching between abstract rules reflects disease severity but not dopaminergic status in Parkinson's disease. Neuropsychologia 47, 1117–1127.
Kiesel, A., Steinhauser, M., Wendt, M., Falkenstein, M., Jost, K., Philipp, A.M., Koch, I., 2010. Control and interference in task switching—a review. Psychol. Bull. 136, 849–874.
Kok, A., 2001. On the utility of P3 amplitude as a measure of processing capacity. Psychophysiology 38, 557–577.
Langbehn, D.R., Brinkman, R.R., Falush, D., Paulsen, J.S., Hayden, M.R., 2004. International Huntington's disease collaborative group. A new model for prediction of the age of onset and penetrance for Huntington's disease based on CAG length. Clin. Genet. 65, 267–277.
Leblois, A., Boraud, T., Meissner, W., Bergman, H., Hansel, D., 2006. Competition between feedback loops underlies normal and pathological dynamics in the basal ganglia. J. Neurosci. 26, 3567–3583.
Marco-Pallares, J., Grau, C., Ruffini, G., 2005. Combined ICA-LORETA analysis of mismatch negativity. Neuroimage 25, 471–477.
Mayr, U., 2001. Age differences in the selection of mental sets: the role of inhibition, stimulus ambiguity, and response-set overlap. Psychol. Aging 16, 96–109.
Mazziotta, J., Toga, A., Evans, A., Fox, P., Lancaster, J., Zilles, K., Woods, R., Paus, T., Simpson, G., Pike, B., et al., 2001. A probabilistic atlas and reference system for the human brain: International Consortium for Brain Mapping (ICBM). Philos. Trans. R. Soc. Lond. B Biol. Sci. 356, 1293–1322.
Monsell, S., 2003. Task switching. Trends Cogn. Sci. 7, 134–140.
Monsell, S., Yeung, N., Azuma, R., 2000. Reconfiguration of task-set: is it easier to switch to the weaker task? Psychol. Res. 63, 250–264.
Münte, T.F., Ridao-Alonso, M.E., Preinfalk, J., Jung, A., Wieringa, B.M., Matzke, M., Dengler, R., Johannes, S., 1997. An electrophysiological analysis of altered cognitive functions in Huntington disease. Arch. Neurol. 54, 1089–1098.
Neuhaus, A.H., Popescu, F.C., Grozea, C., Hahn, E., Hahn, C., Opgen-Rhein, C., Urbanek, C., Dettling, M., 2011. Single-subject classification of schizophrenia by event-related potentials during selective attention. Neuroimage 55, 514–521.
Nicholson, R., Karayanidis, F., Poboka, D., Heathcote, A., Michie, P.T., 2005. Electrophysiological correlates of anticipatory task-switching processes. Psychophysiology 42, 540–554.
Nicholson, R., Karayanidis, F., Davies, A., Michie, P.T., 2006. Components of task-set reconfiguration: differential effects of 'switch-to' and 'switch-away' cues. Brain Res. 1121, 160–176.
Ocklenburg, S., Güntürkün, O., Beste, C., 2011. Lateralized neural mechanisms underlying the modulation of response inhibition processes. Neuroimage 55, 1771–1778.
Pascual-Marqui, R.D., 2002. Standardized low-resolution brain electromagnetic tomography (sLORETA): technical details. Methods Find. Exp. Clin. Pharmacol. 24, 5–12.
Perrin, F., Pernier, J., Bertrand, O., Echallier, J.F., 1989. Spherical splines for scalp potential and current densitiy mapping. Electroencephalogr. Clin. Neurophysiol. 72, 184–187.
Plenz, D., 2003. When inhibition goes incognito: feedback interaction between spiny projection neurons in striatal function. Trends Neurosci. 26, 436–443.
Ranen, N.G., Stine, O.C., Abbott, M.H., Sherr, M., Codori, A.M., Franz, M.L., Chao, N.I., Chung, A.S., Pleasant, N., Callahan, C., 1995. Anticipation and instability of IT-15 (CAG)n repeats in parent-offspring pairs with Huntington disease. Am. J. Hum. Genet. 57, 593–602.
Redgrave, P., Prescott, T.J., Gurney, K., 1999. The basal ganglia: a vertebrate solution to the selection problem? Neuroscience 89, 1009–1023.
Redgrave, P., Rodriguez, M., Smith, Y., Rodriguez-Oroz, M.C., Lehericy, S., Bergman, H., Agid, Y., DeLong, M.R., Obeso, J.A., 2010. Goal-directed and habitual control in the basal ganglia: implications for Parkinson's disease. Nat. Rev. Neurosci. 11, 760–772.
Ridderinkhof, K.R., Ullsperger, M., Crone, E.A., Nieuwenhuis, S., 2004. The role of the medial frontal cortex in cognitive control. Science 306, 443–447.
Roach, B.J., Mathalon, D.H., 2008. Event-related time–frequency analysis: an overview of measures and an analysis of early gamma band phase locking in schizophrenia. Schizophr. Bull. 34, 907–926.
Rogers, R.D., Monsell, S., 1995. The costs of a predictable switch between simple cognitive tasks. J. Exp. Psychol. Gen. 124, 207–231.
Rosas, H.D., Salat, D.H., Lee, S.Y., Zaleta, A.K., Pappu, V., Fischl, B., Greve, D., Hevelone, N., Hersch, S.M., 2008. Cerebral cortex and the clinical expression of Huntington's disease: complexity and heterogeneity. Brain 131, 1057–1068.
Rushworth, M., Hadland, K.A., Paus, T., Sipila, P.K., 2002. Role of the human medial frontal cortex in task switching: a combined fMRI and TMS study. J. Neurophysiol. 57, 2577–2592.
Sammer, G., Blecker, C., Gebhardt, H., Bischoff, M., Stark, R., Morgen, K., Vaitl, D., 2007. Relationship between regional hemodynamic activity and simultanously recorded EEG-theta associated with mental arithmetic-induced workload. Hum. Brain Mapp. 28, 793–803.
Sauseng, P., Griesmayr, B., Freunberger, R., Klimesch, W., 2010. Control mechanisms in working memory: a possible function of EEG theta oscillations. Neurosci. Biobehav. Rev. 34, 1015–1022.
Schneider, D.W., Anderson, J.R., 2010. Asymmetric switch costs as sequential difficulty effects. Q. J. Exp. Psychol. (Hove) 63, 1873–1894.
Sekihara, K., Sahani, M., Nagarajan, S.S., 2005. Localization bias and spatial resolution of adaptive and non-adaptive spatial filters for MEG source reconstruction. Neuroimage 25, 1056–1067.
Siesling, S., van Vugt, J.P., Zwinderman, K.A., Kieburtz, K., Roos, R.A., 1998. Unified Huntington's disease rating scale: a follow up. Mov. Disord. 13, 915–919.
Smith, E.E., Jonides, J., 1999. Storage and executive processes in the frontal lobes. Science 283, 1657–1661.
Surmeier, J.D., Ding, J., Day, M., Wang, Z., Shen, W., 2007. D1 and D2 dopamine-receptor modulation of striatal glutamatergic signalling in striatal medium spiny neurons. Trends Neurosci. 30, 228–235.
Tabrizi, S.J., Langbehn, D.R., Leavitt, B.R., Roos, R.A., Durr, A., Craufurd, D., Kennard, C., Hicks, S.L., Fox, N.C., Scahill, R.I., et al., 2009. Biological and clinical manifestation of Huntington's disease in the longitudinal TRACK-HD study: cross-sectional analysis of baseline data. Lancet Neurol. 8, 791–801.
Tallon-Baudry, C., Bertrand, O., Delpuech, C., Pernier, J., 1997. Oscillatory gamma-band (30–70 Hz) activity induced by a visual search task in humans. J. Neurosci. 17, 722–734.
Thomas, E.A., Coppola, G., Tang, B., Kuhn, A., Kim, S., Geschwind, D.H., et al., 2011. In vivo cell-autonomous transcriptional abnormalities revealed in mice expressing mutant huntingtin in striatal but not cortical neurons. Hum. Mol. Genet. 20, 1049–1060.
van Oostrom, J.C., Dekker, M., Willemsen, A.T., de Jong, B.M., Roos, R.A., Leenders, K.L., 2009. Changes in striatal dopamine D2 receptor binding in pre-clinical Huntington's disease. Eur. J. Neurol. 16, 226–231.
van Veen, V., Carter, C.S., 2002. The anterior cingulate as a conflict monitor: fMRI and ERP studies. Physiol. Behav. 77, 477–482.
Verleger, R., Hagenah, J., Weiss, M., Ewers, T., Heberlein, I., Pramstaller, P.P., Siebner, H.R., Klein, C., 2010. Responsiveness to distracting stimuli, though increased in Parkinson's disease, is decreased in asymptomatic PINK1 and Parkin mutation carriers. Neuropsychologia 48, 467–476.
Vitacco, D., Brandeis, D., Pascual-Marqui, R., Martin, E., 2002. Correspondence of event-related potential tomography and functional magnetic resonance imaging during language processing. Hum. Brain Mapp. 17, 4–12.
Whitwell, J.L., Crum, W.R., Watt, C., Fox, N.C., 2001. Normalization of cerebral volumes by use of intracranial volume: implications for longitudinal quantitative MR imaging. AJNR Am. J. Neuroradiol. 22, 1483–1489.
Willemssen, R., Müller, T., Schwarz, M., Falkenstein, M., Beste, C., 2009. Response monitoring in de novo patients with Parkinson's disease. PLoS One e4898.
Willemssen, R., Falkenstein, M., Schwarz, M., Müller, T., Beste, C., 2011. Effects of aging, Parkinson's disease, and dopaminergic medication on response selection and control. Neurobiol. Aging 32, 327–335.
Wylie, G., Allport, A., 2000. Task switching and the measurement of "switch costs". Psychol. Res. 63, 212–233.
Yordanova, J., Falkenstein, M., Hohnsbein, J., Kolev, V., 2004. Parallel systems of error processing in the brain. Neuroimage 22, 590–602.